

Single-pixel digital holography with phase-encoded illumination

LLUÍS MARTÍNEZ-LEÓN,^{1,*} PERE CLEMENTE,² YUTAKA MORI,³ VICENT CLIMENT,¹ JESÚS LANCIS,¹ AND ENRIQUE TAJAHUERCE¹

¹GROC-UJI, Institute of New Imaging Technologies (INIT), Universitat Jaume I, 12071 Castelló de la Plana, Spain

²Servei Central d'Instrumentació Científica (SCIC), Universitat Jaume I, 12071 Castelló de la Plana, Spain

³Faculty of Engineering, Kagawa University, Kagawa 761-0322, Japan

*lluis.martinez@uji.es

Abstract: We demonstrate imaging of complex amplitude objects through digital holography with phase-structured illumination and bucket detection. The object is sampled with a set of micro-structured phase patterns implemented onto a liquid-crystal spatial light modulator while a bucket detector sequentially records the irradiance fluctuations corresponding to the interference between object and reference beams. Our reconstruction algorithm retrieves the unknown phase information from the full set of photocurrent measurements. Interestingly, the sampling functions can be codified onto the reference beam, so they can be nonlocal with respect to the object. Finally, we show that the system is well-fitted for transmission of the object information through scattering media.

© 2017 Optical Society of America

OCIS codes: (090.1995) Digital holography; (110.0110) Imaging systems; (110.0113) Imaging through turbid media; (110.1758) Computational imaging; (120.5050) Phase measurement.

References and links

1. P. Török and F.-J. Kao, eds., *Optical Imaging and Microscopy* (Springer, 2007).
2. G. Popescu, *Quantitative phase imaging of cells and tissues* (Mc Graw-Hill, 2011).
3. P. Ferraro, A. Wax, and Z. Zalevsky, eds., *Coherent Light Microscopy* (Springer, 2011).
4. T. Latychevskaia, J.-N. Longchamp, and H.-W. Fink, "When holography meets coherent diffraction imaging," *Opt. Express* **20**(27), 28871–28892 (2012).
5. G. Zheng, R. Horstmeyer, and C. Yang, "Wide-field, high-resolution Fourier ptychographic microscopy," *Nat. Photonics* **7**(9), 739–745 (2013).
6. U. Schnars and W. P. O. Jüptner, "Digital recording and numerical reconstruction of holograms," *Meas. Sci. Technol.* **13**(9), R85–R101 (2002).
7. I. Yamaguchi and T. Zhang, "Phase-shifting digital holography," *Opt. Lett.* **22**(16), 1268–1270 (1997).
8. Y. Awatsuji, M. Sasada, and T. Kubota, "Parallel quasi-phase shifting digital holography," *Appl. Phys. Lett.* **85**(6), 1069–1071 (2004).
9. L. Martínez-León, M. Araiza-E, B. Javidi, P. Andrés, V. Climent, J. Lancis, and E. Tajahuerce, "Single-shot digital holography by use of the fractional Talbot effect," *Opt. Express* **17**(15), 12900–12909 (2009).
10. T. Nomura and M. Imbe, "Single-exposure phase-shifting digital holography using a random-phase reference wave," *Opt. Lett.* **35**(13), 2281–2283 (2010).
11. M. F. Duarte, M. A. Davenport, D. Takhar, J. N. Laska, Ting Sun, K. F. Kelly, and R. G. Baraniuk, "Single-pixel imaging via compressive sampling," *IEEE Signal Process. Mag.* **25**(2), 83–91 (2008).
12. G. A. Howland, D. J. Lum, M. R. Ware, and J. C. Howell, "Photon counting compressive depth mapping," *Opt. Express* **21**(20), 23822–23837 (2013).
13. E. Tajahuerce, V. Durán, P. Clemente, E. Irlés, F. Soldevila, P. Andrés, and J. Lancis, "Image transmission through dynamic scattering media by single-pixel photodetection," *Opt. Express* **22**(14), 16945–16955 (2014).
14. V. Durán, F. Soldevila, E. Irlés, P. Clemente, E. Tajahuerce, P. Andrés, and J. Lancis, "Compressive imaging in scattering media," *Opt. Express* **23**(11), 14424–14433 (2015).
15. C. M. Watts, D. Shrekenhamer, J. Montoya, G. Lipworth, J. Hunt, T. Sleasman, S. Krishna, D. R. Smith, and W. J. Padilla, "Terahertz compressive imaging with metamaterial spatial light modulators," *Nat. Photonics* **8**(8), 605–609 (2014).
16. E. J. Candes and M. B. Wakin, "An introduction to compressive sampling," *IEEE Signal Process. Mag.* **25**(2), 21–30 (2008).
17. A. Gatti, E. Brambilla, and L. A. Lugiato, "Quantum imaging," *Prog. Opt.* **51**, 251–348 (2008).
18. J. H. Shapiro, "Computational ghost imaging," *Phys. Rev. A* **78**, 061802(R) (2008).

19. Y. Bromberg, O. Katz, and Y. Silberberg, "Ghost imaging with a single detector," *Phys. Rev. A* **79**(5), 053840 (2009).
20. N. Radwell, K. J. Mitchell, G. M. Gibson, M. P. Edgar, R. Bowman, and M. J. Padgett, "Single-pixel infrared and visible microscope," *Optica* **1**(5), 285–289 (2014).
21. Y. Wu, P. Ye, I. O. Mirza, G. R. Arce, and D. W. Prather, "Experimental demonstration of an optical-sectioning compressive sensing microscope (CSM)," *Opt. Express* **18**(24), 24565–24578 (2010).
22. A. D. Rodríguez, P. Clemente, E. Tajahuerce, and J. Lancis, "Dual-mode optical microscope based on single-pixel imaging," *Opt. Lasers Eng.* **82**, 87–94 (2016).
23. V. Durán, P. Clemente, M. Fernández-Alonso, E. Tajahuerce, and J. Lancis, "Single-pixel polarimetric imaging," *Opt. Lett.* **37**(5), 824–826 (2012).
24. S. S. Welsh, M. P. Edgar, R. Bowman, B. Sun, and M. J. Padgett, "Near video-rate linear Stokes imaging with single-pixel detectors," *J. Opt.* **17**(2), 025705 (2015).
25. V. Studer, J. Bobin, M. Chahid, H. S. Mousavi, E. Candes, and M. Dahan, "Compressive fluorescence microscopy for biological and hyperspectral imaging," *Proc. Natl. Acad. Sci. U.S.A.* **109**(26), E1679–E1687 (2012).
26. F. Soldevila, E. Irlles, V. Durán, P. Clemente, M. Fernández-Alonso, E. Tajahuerce, and J. Lancis, "Single-pixel polarimetric imaging spectrometer by compressive sensing," *Appl. Phys. B* **113**(4), 551–558 (2013).
27. N. Huynh, E. Zhang, M. Betcke, S. Arridge, P. Beard, and B. Cox, "Single-pixel optical camera for video rate ultrasonic imaging," *Optica* **3**(1), 26–29 (2016).
28. V. Ntziachristos, "Going deeper than microscopy: the optical imaging frontier in biology," *Nat. Methods* **7**(8), 603–614 (2010).
29. A. P. Mosk, A. Lagendijk, G. Leroose, and M. Fink, "Controlling waves in space and time for imaging and focusing in complex media," *Nat. Photonics* **6**(5), 283–292 (2012).
30. Y.-K. Xu, W. T. Liu, E. F. Zhang, Q. Li, H. Y. Dai, and P. X. Chen, "Is ghost imaging intrinsically more powerful against scattering?" *Opt. Express* **23**(26), 32993–33000 (2015).
31. M. Bina, D. Magatti, M. Molteni, A. Gatti, L. A. Lugiato, and F. Ferri, "Backscattering differential ghost imaging in turbid media," *Phys. Rev. Lett.* **110**(8), 083901 (2013).
32. M. J. Purcell, M. Kumar, S. C. Rand, and V. Lakshminarayanan, "Holographic imaging through a scattering medium by diffuser-aided statistical averaging," *J. Opt. Soc. Am. A* **33**(7), 1291–1297 (2016).
33. A. K. Singh, D. N. Naik, G. Pedrini, M. Takeda, and W. Osten, "Looking through a diffuser and around an opaque surface: a holographic approach," *Opt. Express* **22**(7), 7694–7701 (2014).
34. T.-C. Poon, "Optical scanning holography: a review of recent progress," *J. Opt. Soc. Korea* **13**(4), 406–415 (2009).
35. P. W. M. Tsang, T.-C. Poon, J.-P. Liu, T. Kim, and Y. S. Kim, "Low complexity compression and speed enhancement for optical scanning holography," *Sci. Rep.* **6**, 34724 (2016).
36. A. C. S. Chan, K. K. Tsia, and E. Y. Lam, "Subsampled scanning holographic imaging (SuSHI) for fast, non-adaptive recording of three-dimensional objects," *Optica* **3**(8), 911–917 (2016).
37. D. J. Brady, K. Choi, D. L. Marks, R. Horisaki, and S. Lim, "Compressive holography," *Opt. Express* **17**(15), 13040–13049 (2009).
38. Y. Rivenson, A. Stern, and B. Javidi, "Compressive Fresnel holography," *J. Disp. Technol.* **6**(10), 506–509 (2010).
39. M. M. Marim, M. Atlan, E. Angelini, and J.-C. Olivo-Marin, "Compressed sensing with off-axis frequency-shifting holography," *Opt. Lett.* **35**(6), 871–873 (2010).
40. P. Clemente, V. Durán, E. Tajahuerce, P. Andrés, V. Climent, and J. Lancis, "Compressive holography with a single-pixel detector," *Opt. Lett.* **38**(14), 2524–2527 (2013).
41. P. Clemente, V. Durán, E. Tajahuerce, V. Torres-Company, and J. Lancis, "Single-pixel digital ghost holography," *Phys. Rev. A* **86**, 041803 (2012).
42. G. Rousseau and A. Blouin, "Hadamard multiplexing in laser ultrasonics," *Opt. Express* **20**(23), 25798–25816 (2012).
43. B. Sun, M. P. Edgar, R. Bowman, L. E. Vittert, S. Welsh, A. Bowman, and M. J. Padgett, "3D computational imaging with single-pixel detectors," *Science* **340**(6134), 844–847 (2013).
44. E. Candes, J. Romberg, and T. Tao, "Robust uncertainty principles: Exact signal reconstruction from highly incomplete frequency information," *IEEE Trans. Inf. Theory* **52**(2), 489–509 (2006).
45. D. Donoho, "Compressed sensing," *IEEE Trans. Inf. Theory* **52**(4), 1289–1306 (2006).
46. F. Soldevila, E. Salvador-Balaguer, P. Clemente, E. Tajahuerce, and J. Lancis, "High-resolution adaptive imaging with a single photodiode," *Sci. Rep.* **5**, 14300 (2015).
47. F. Soldevila, P. Clemente, E. Tajahuerce, N. Uribe-Patarroyo, P. Andrés, and J. Lancis, "Computational imaging with a balanced detector," *Sci. Rep.* **6**, 29181 (2016).
48. W. Pratt, J. Kane, and H. C. Andrews, "Hadamard transform image coding," *Proc. IEEE* **57**(1), 58–68 (1969).

1. Introduction

Developing a smart and efficient approach to recover the complex-valued amplitude of the diffraction pattern that emerges from an object has been one of the most attractive challenges in imaging science since the early times of modern optical microscopy and Zernike's phase-

contrast method. Indeed, by means of a variety of techniques, phase imaging can retrieve information not directly available through square-law detectors, that is to say, not accessible with simple intensity measurements [1–3]. Phase information is essential for studying complex-valued objects, including transparent samples, as a myriad of biological specimens whose features may only be revealed by phase methods. Among phase imaging methods, iterative techniques such as coherent diffraction imaging or ptychography provide improved spatial resolution [4] and expanded field of view [5], but oversampling and a non-negligible computational effort are required. Digital holography is nowadays a well established method for simultaneous phase and amplitude imaging [6], with straightforward procedures for the reconstruction of complex diffraction patterns. In particular, phase-shifting digital holography [7] is an interesting procedure to exploit efficiently the spatial resolution of digital sensors, especially with the application of parallel approaches [8–10].

On the other hand, over the past few years a number of researchers have focused their interest on different innovative computational imaging techniques such as single-pixel imaging with microstructured illumination [11]. Imaging techniques with single-pixel detectors offer a series of advantages in those applications limited by scarce illumination [12], involving vision through scattering media [13,14], or working in spectral ranges where it is difficult to employ detectors with a 2D structure [15]. In particular, single-pixel imaging benefits from the multiplexing operation (Fellgett's advantage) in measurements limited by noise sources which are independent of the signal. This advantage is therefore more relevant in the infrared spectral band. Single-pixel imaging is also well adapted to apply compressive sensing algorithms reducing in this way the measurement time [11,16].

At the heart of this technique is the fact that the stage of spatial sampling is shifted away from the sensor to a set of microstructured spatial masks that are codified onto a programmable spatial light modulator. The masks are optically projected onto the sample and the whole intensity is collected by a bucket (single-pixel) sensor. Measurements are performed sequentially by changing the spatial mask. If many different masks are used, their shapes and the intensity signals are combined to retrieve the sample. The resolution of the reconstructed image is directly depending on the resolution of the projecting patterns. The technique is closely related to ghost imaging, which also uses single-pixel detectors to reconstruct images based on the correlation between two signals [17]. In particular it is analogous to computational ghost imaging, where a sequence of deterministic random patterns is used for sampling the object [18,19]. However, computational ghost imaging requires coherent light illumination while conventional single-pixel imaging approaches are able to work with totally incoherent light sources.

Single-pixel imaging has been applied in different optical imaging procedures including, among others, microscopy [20–22], polarization imaging [23,24], hyperspectral imaging [25,26], ultrasound field mapping [27] or 3D imaging [12]. The integration of single-pixel methods with other singular imaging techniques remains a wide field to explore, raising expectations on new applications. One of these techniques could be imaging through scattering media [28,29]. Imaging techniques based on microstructured illumination and single-pixel detection have shown already to be an efficient method to image objects through scattering media even in the dynamic case and with objects completely embedded in the medium [13,14]. Imaging over scattering media has been also reported in ghost imaging [30,31]. In this direction, recently, a simple and straightforward holographic imaging method has been proposed to record digital holograms through scattering media [32,33].

Some approaches have been reported regarding single-pixel imaging or compressive sensing in the field of digital holography. In optical scanning holography [34–36], as a time-varying Fresnel zone plate is displayed onto each point of the object scene, a photodetector collects all the diffracted light. Once the object is scanned, the hologram can be obtained through an electronic process. With a different perspective, other digital holography approaches offer insight about the relation between holography recording and compressive

sampling procedures [37–39]. On the other hand, our group reported a system based on single-pixel detection for recording digital holograms with a reduced number of measurements [40], where the object was sampled with intensity Hadamard patterns, not with phase-codified functions. A computational ghost holography technique has also been reported [41] but sampling the object with random speckle patterns. In spite of the expected capability of phase masks to enhance the signal-to-noise ratio of photocurrent measurements, they have not been previously reported in single-pixel digital holography since they require either phase sensitive measurements or differential detection.

In this paper, we present a new method for retrieving the complex information of an object by combining phase-structured illumination with single-pixel detection techniques and phase-shifting digital holography. Our approach benefits both from the enthralling properties of single-pixel imaging techniques and the flexibility and efficiency of phase-shifting holography, providing several advantages. Firstly, by using microstructured sampling patterns which are encoded in phase, our system would be expected to benefit from an enhancement by a factor of 2 in the signal-to-noise ratio when compared to the widely adopted amplitude modulation schemes. Actually, improvements in the signal-to-noise ratio for phase-encoded Hadamard patterns have been already reported in the terahertz domain and in laser ultrasonic applications [15,42]. Second, we can codify the phase steps necessary to apply phase-shifting techniques and the phase sampling patterns in the same spatial light modulator (SLM). This simplifies the optical system when comparing to previous approaches, as only one phase modulator is used. Third, we employ a very simple Michelson configuration, more stable than previous interferometric setups used for single-pixel digital holography. Finally, we take advantage of the fact that single-pixel imaging barely depends on the optical system existing after the object, which allows the transmission of the object information through turbid media.

The remaining of the paper is structured as follows. Section 2 recalls the main features of single-pixel imaging. Section 3 presents the principles of our new approach for complex-value encoded single-pixel phase imaging, with an experimental implementation shown in Section 4. Proof-of-concept results are presented in Section 5. Finally, we address some concluding remarks.

2. Single-pixel imaging

Unlike other conventional approaches using a 2D sensor, in single-pixel imaging, a simple photodiode collects the light intensity codifying the information of interest, while the 2D spatial sampling is introduced elsewhere in the system. Typically, the data to be recorded are the photocurrent fluctuations corresponding to sampling the scene with different microstructured patterns, which are implemented sequentially onto an SLM.

In short, single-pixel imaging seeks the optical reconstruction of an intensity object $t(\vec{r})$, through the projection of a set of sampling patterns $m_i(\vec{r})$, with $i = 1, 2, \dots, N$, and the recording of the resulting values of total irradiance. In the conventional implementation, the sampling functions are real and positive. Also, binary patterns are preferred. In this way, they can be easily implemented using a fast digital micromirror device (DMD). Concerning the type of measurement patterns, various sampling functions can be employed. For instance, raster-scan style masks stem from the well-known raster-scan technique in which single spatial pixels are measured sequentially. Random masks can also be used, in which each pattern has a random distribution of binary values [43]. In our approach, we use Hadamard patterns, which are easily implemented and provide minimum variance least-squares estimation of the unknown variables [15]. Hadamard patterns are generated from the Hadamard-Walsh functions, representing modulation in both horizontal and vertical directions. As an example, Hadamard masks for a 2×2 pixels image are shown in Fig. 1,

where the white color represents the +1 value, and the black zones the -1 value (or the phase 0 and π , respectively).



Fig. 1. Hadamard masks for a 2×2 dimension.

In the experiment, I_i , the irradiance transmitted through the sample for the sampling pattern i , is recorded with a single-pixel detector after the output light beam has been concentrated on it. In mathematical terms, the integrated intensity can be written as

$$I_i \propto \iint |t(\vec{r})m_i(\vec{r})|^2 d^2\vec{r}. \quad (1)$$

Subsequently, the partial variations of the irradiance through the object are reconstructed through the linear superposition of the sampling functions weighted with the recorded photocurrents; i.e.,

$$|t(\vec{r})|^2 = \sum_i I_i m_i(\vec{r}). \quad (2)$$

Although recording and reconstruction is a time-consuming process, single-pixel cameras are well adapted for compressed sensing [16,44,45]. Compressive sensing techniques merge the sampling with the compression process, instead of recording a considerable amount of information which would be mostly discarded afterwards. Also, adaptive compressive sensing or complementary detection using a balanced detector can be used to speed up the sensing stage [46,47]. In this way, it has been demonstrated operation at frame rates of the order of tens of frames per second, though with low spatial resolution.

3. Complex-value encoded single-pixel phase imaging

Here, we consider the extension of the above procedures to phase measurements with coherent light. A holographic single-pixel detection arrangement, consisting of a compact phase-shifting Michelson interferometer, is proposed. The system combines the phase-shifting interferometer with a single-pixel detection arrangement with complex-value encoded illumination, which is one step further from previous single-pixel digital holography approaches. In the measurement procedure, binary phase Hadamard masks with phase values 0 and π are displayed onto the object by means of a spatial light modulator. The interference pattern produced by the coherent sum of light coming from the object and from a reference beam is integrated by a photodiode. In order to obtain a complete reconstruction, several measurements are performed for each Hadamard pattern with a different global phase-shift between the object and the reference beams. If the object $t(\vec{r})$ is sampled with complex-valued patterns $m_i(\vec{r})$ and a phase-shift φ is introduced in the reference arm, with an amplitude distribution $R(\vec{r})$, then the irradiance measurement I_i corresponding to each interference pattern can be expressed as

$$I_{i,\varphi} \propto \iint |t(\vec{r})m_i(\vec{r}) + e^{j\varphi}R(\vec{r})|^2 d^2\vec{r}. \quad (3)$$

Four photocurrent values are then registered for each sampling pattern, one for each phase-shift ($\varphi = 0, \pi/2, \pi$ and $3\pi/2$). In essence, the measurement process can be understood as the projection of the object scene in the basis of 2D functions defined by the phase Hadamard patterns, by means of a phase-shifting process. For each sampling pattern, the complex

coefficient associated to the pattern can be obtained from the phase-shifted photocurrents as follows:

$$y_i = \frac{1}{4|R|} \left[(I_{i,0} - I_{i,\pi}) + j(I_{i,3\pi/2} - I_{i,\pi/2}) \right], \quad (4)$$

where the amplitude of the reference wave has been considered as a constant. This expression represents the extension of the standard phase-shifting algorithm for spatial light distributions in conventional digital holography [7] to integrated intensities in single-pixel digital holography [40]. The complex amplitude distribution of the object is retrieved through the linear superposition:

$$t(\vec{r}) = \sum_i y_i m_i(\vec{r}). \quad (5)$$

The object reconstruction can be interpreted as the superposition of the basis functions, the phase Hadamard patterns, weighted by their corresponding complex coefficients, which are calculated from the phase-shifting algorithm in Eq. (4). In fact, the measurement process performed by using Eqs. (3) and (4) can be understood as a change of basis which is later reversed by using Eq. (5). We would like to emphasize that in contrast with conventional single-pixel imaging techniques, the coefficients associated to the Hadamard patterns are complex values. It is also worth remarking that substituting Eq. (4) into Eq. (5) provides an alternative insight of our imaging procedure and a different way to process the recorded information. In this new approach, single-pixel imaging techniques can be first applied to obtain the spatial distribution of each phase-shifted interferogram separately. Afterwards, the complex object is obtained by applying conventional phase-shifting algorithm to the computed interferograms, instead of calculating a single multiplexed reconstruction with complex coefficients.

It is important to note that the 2D complex amplitude distribution reconstructed by Eq. (5) corresponds to that located at the plane sampled by the Hadamard phase patterns. For simplicity, in this work we consider that the phase patterns are specifically projected onto the object plane and, therefore, the object distribution is reconstructed directly, as an image hologram in conventional holographic imaging, without any need of considering light propagation. However, by projecting the Hadamard phase patterns onto a different plane, we would be able to measure the complex amplitude distribution of different Fresnel diffraction patterns by single-pixel detection. As in conventional Fresnel holography, in this case, the retrieved distribution should be propagated with the diffraction formula to find the object distribution.

Note that in our interferometric optical system, the difference between sampling the object with micro-structured light patterns, commonly named active imaging, or imaging the object at the plane where the sampling patterns are codified, passive imaging, is not relevant as both situations will provide indistinguishable input diffraction patterns. Interestingly, a similar result is obtained when the sampling phase patterns are projected not in the object path of the interferometer but in the reference path. In particular, let us consider that the set of Hadamard phase patterns are projected in the reference path but at the same distance from the light detector than the object. In this case, it can be shown that the integrated interference between the light diffracted by the object and the modulated reference beam is

$$I_{i,\varphi} \propto \iint \left| t(\vec{r}) + e^{i\varphi} m_i(\vec{r}) R(\vec{r}) \right|^2 d^2\vec{r}, \quad (6)$$

which provides the same photocurrent measurements as Eq. (3). This property allows us to design a very compact single-pixel holographic setup, as both the Hadamard phase patterns codifying the 2D sampling masks and the constant phases used to apply phase-shifting algorithms can be displayed at the same time in a single SLM located at the reference arm of

the interferometer. This provides high flexibility to the system, as the modulating device remains now in the reference beam, leaving the object beam unperturbed. Furthermore, our system is then well adapted to employ a stable Michelson interferometer architecture.

One of the capabilities of our phase-encoded imaging method concerns the transmission of the object information through scattering media, and it is based on an interesting property of single-pixel cameras [13,14]. In this context, image reconstruction can be explained by the high correlation between the spatial sampling patterns displayed over the object and the photocurrent values recorded by a photodiode. In particular, for our system, the high correlation between the phase Hadamard patterns displayed by the SLM and the integrated photocurrent value at the interferometer output is the key point to obtain the final complex image. And satisfyingly, this correlation does not change when a scattering medium is interposed before the detector because, although the light is spatially spread, the intensity arriving to the photodetector is still proportional to that obtained without the diffuser. As shown experimentally below, hologram reconstruction is possible with single-pixel techniques even when a scattering media is located in front of the detector.

4. Experimental set-up

The experimental set-up based on a Michelson interferometer is shown in Fig. 2. The light source was a 532 nm fiber-coupled solid state laser (Oxxius OXX-532-50-COL-SLM). We have employed a liquid crystal on silicon SLM (Hamamatsu X10468-4), with a resolution of 792×600 pixels, and a pixel pitch of $20 \mu\text{m}$. The detector was the Thorlabs photodiode DET36A/M.

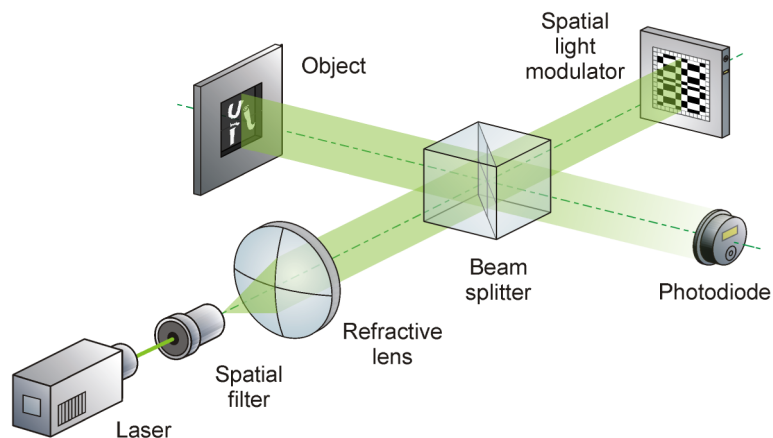


Fig. 2. Experimental set-up.

For recording a hologram, the SLM displayed a composite phase pattern encoding simultaneously a) a Hadamard phase pattern, b) the relative phase between reference and object beam for phase shifting, and c) the correction of the optical aberrations previously measured in the system, mainly due to the curvature of the modulator's backplane. Hadamard patterns were codified as binary phase masks, with 0 and π values, but the resultant phase modulation was wrapped, restricted to the interval from 0 to 2π . In these experiments, we have dealt with an image resolution of 64×64 pixels, corresponding to a total amount of 4096 sampling patterns for a standard single-pixel reconstruction. In the SLM, we represented the measurement patterns by using 8×8 SLM pixels for each sampling pixel. We applied the usual 4-step phase-shifting technique for each one of the patterns displayed, in order to obtain the complex coefficient corresponding to each basis function from the photocurrent value recorded for each phase-shift.

In our single-pixel measurements, object and SLM were placed at the same distance from the detector and, as a consequence, the retrieved image represents what in conventional digital holography is called an image plane hologram. Thus, light propagation from the final hologram to the object plane does not need to be considered to obtain the image. The reconstruction algorithm for obtaining the hologram consisted of the superposition of a limited number of Hadamard patterns, as shown in Eq. (5), using the coefficients computed with Eq. (4) as weighting factors. In our procedure, no convex minimization algorithms have been applied, since the partial set of Hadamard patterns employed for sampling, corresponding to low Hadamard “frequencies”, has provided a proper object reconstruction. The information provided by the photocurrent coefficients of these low Hadamard “frequencies” is enough for reconstructing the main features of the images. The interpretation of frequency in this context is related to the number of changes of sign in the Hadamard matrices [48], that is to say, the amount of changes of phase in the vertical or horizontal dimensions in the sampling patterns.

5. Experimental results

Firstly, we show the result of the reconstruction of an amplitude transparency, the logo of our university, attached to a mirror. The object and the SLM are located at the same distance from the detector in the object and reference arms, respectively, of the interferometer, as shown in Fig. 2. In this configuration, phase-encoding is performed in the reference beam. In Fig. 3 (right), we show the image corresponding to the reconstruction of the object amplitude after recording the hologram with our single-pixel system. We use Hadamard phase functions with a resolution of 64×64 pixels and, therefore, this is the maximum resolution of the final image. However, to speed the process, we send only a 40% of the total number of Hadamard functions. We also present an image of the object plane recorded directly by a conventional 2D sensor (Fig. 3, left), an Allied Stingray camera, F-145B, with a pixel size of $6.45 \mu\text{m}$. The resolution of this image has been adjusted to 64×64 pixels.

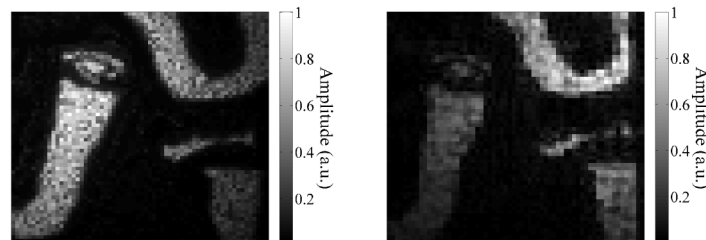


Fig. 3. Conventional direct imaging (left) and single-pixel hologram reconstruction (right) of an amplitude object.

Next, we present results showing the reconstruction of a phase-object. For this experiment, the set-up has been slightly modified in order to display a phase object in the SLM. Now, in addition to the phase information mentioned above (backplane curvature correction, sampling patterns and phase shifts), the SLM also displays our phase object, an 8-bit phase image of the Universitat Jaume I logo. The roles of reference and object arms have been exchanged in the set-up, and just a mirror lies in the position where the object is placed in Fig. 2. Thus, in this specific case, phase-encoded patterns are modulated in the object beam.

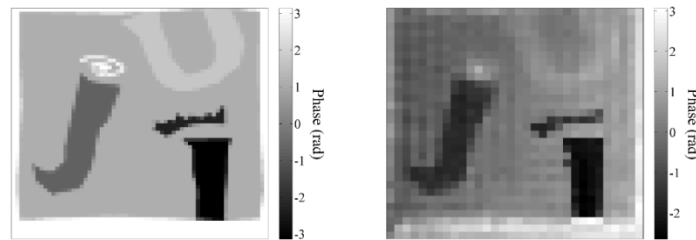


Fig. 4. 64×64 pixel original image (left) and single-pixel hologram reconstruction (right) of a phase object displayed onto the SLM.

Figure 4 (right) shows the reconstructed phase with our single-pixel system, obtained with the phase-shifting algorithm. Just 20% of the Hadamard functions corresponding to an image resolution of 64×64 pixels have been used. For comparison, in Fig. 4 (left), the original phase image, with a resolution of 64×64 pixels is shown. With the reconstruction of the phase object displayed in the SLM, the capability of the system for retrieving phase information through a digital holography single-pixel procedure with phase-encoded sampling patterns is demonstrated.

We have also tested the capability of our system to transmit object information through a scattering medium. To this end, we have performed a similar experiment to the first one but this time we have inserted a diffuser, a rough solid plastic, placed approximately 10 cm before the detector, as shown in Fig. 5.

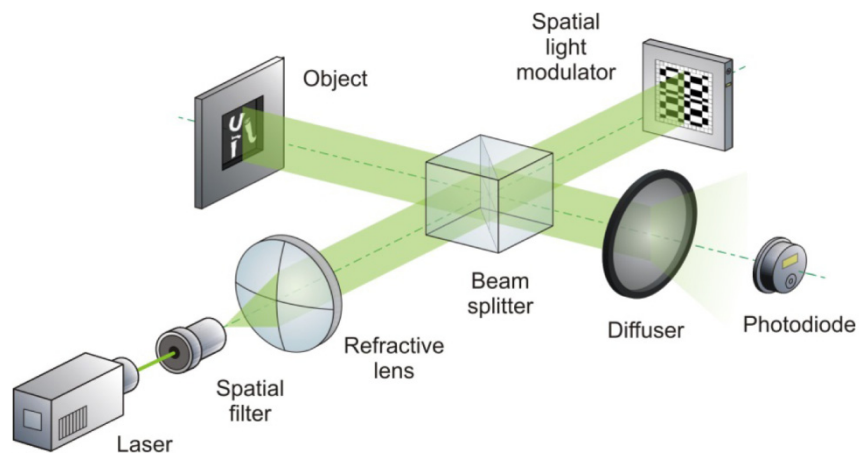


Fig. 5. Experimental set-up for phase imaging through a diffuser.

Figure 6 (right) shows the amplitude reconstruction of the image through our single-pixel camera, with a quality comparable to the image without diffuser. Also in Fig. 6 (left) we show the image obtained with a conventional camera, where no feature of the UJI logo can be identified. The possible differences between single-pixel reconstructions without or through the diffuser, comparing Fig. 3 and Fig. 6, may be originated by the reduction in light intensity reaching the detector in the latter case. For the results both without or with diffuser, it is worth mentioning that the accuracy expected is lower than the original 64×64 pixels, because just a fraction of the sampling patterns corresponding to that resolution have been used.

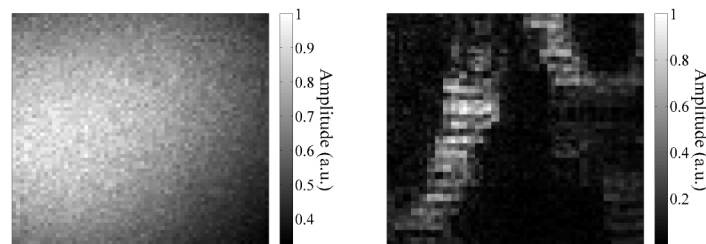


Fig. 6. Conventional direct imaging (left) and single-pixel hologram reconstruction (right) of an amplitude object, through a diffuser.

Some difficulties have appeared in the experimental implementation of our approach, mainly related to stability issues, which have been fixed with the use of a SLM with reduced phase flickering. In fact, when a high number of sampling patterns were used and several intensities were measured for averaging, the time needed for retrieving a holographic image was in the order of minutes. For minimizing these issues, a fast measurement process, by using other kinds of modulation devices, such as ferroelectric liquid crystal displays or digital micromirror devices, could be considered.

6. Conclusions

Recent results on single-pixel digital holography concerning the reconstruction of the amplitude and phase of an object by using complex-encoded masks together with phase-shifting techniques have been presented. We have designed a compact system where the micro-structured illumination sampling the object has been codified in phase, improving light efficiency. Experimental results show the feasibility of the method and the advantages of using phase-codification and single-pixel imaging. The versatility of the system is high, with just one modulation device, which is placed not in the object but in the reference arm of the interferometer. The diffraction pattern to be recorded with our single-pixel holographic system can be selected by adjusting the plane where sampling patterns are displayed. This selection can be done by simply shifting the position of the SLM, where the Hadamard phase patterns are displayed, to the required plane. Our results also include the holographic reconstruction of images with a scattering medium located before the detector, thanks to the properties of single-pixel detection techniques, with a quality comparable to those obtained when the scattering medium is absent.

Funding

Spanish Ministerio de Economía y Competitividad (project FIS2013-40666-P), Generalitat Valenciana (project PROMETEO 2016-079) and Universitat Jaume I (project P1·1B2015-35).

Acknowledgments

We are very grateful to Hamamatsu Photonics for providing the LCoS SLM used in our experiments.